DSWIPT Scheme for Cooperative Transmission in Downlink NOMA System

Kai Yang, Xiao Yan(✉), Qian Wang, Kaiyu Qin, and Dingde Jiang

School of Aeronautics and Astronautics,
University of Electronic Science and Technology of China, Chengdu 611731, China
yanxiao@uestc.edu.cn

Abstract. In this paper, we focus on the issue how to reduce the throughput performance gap between the cell-center user and the cell-edge user in a downlink two-user non-orthogonal multiple access (NOMA) system. To this end, we apply the Simultaneous Wireless Information and Power Transfer (SWIPT) protocol to the NOMA scheme and propose a dynamic SWIPT (DSWIPT) cooperative NOMA scheme, in which both the time allocation (TA) ratio and power splitting (PS) ratio can be adjusted dynamically to improve the performance of the cell-edge user in the system. Specifically, we derive two analytical expressions for the outage probability (OP) of the cell-center user and the cell-edge user to study the DSWIPT NOMA scheme's influence on the system. And we also propose an optimization algorithm to find the optimal TA ratio and PS ratio for maximizing the sum-throughput of the system. The numerical results show that the analytical results are in accordance with the Monte-Carlo simulation results exactly and the DSWIPT NOMA scheme has a better performance in both the sum-throughput of the system and the OP of the cell-edge user comparing with the non-cooperative NOMA scheme and the SWIPT NOMA scheme.

Keywords: Non-orthogonal multiple access (NOMA) · Dynamic simultaneous wireless information and power transfer (DSWIPT) · Time allocation ratio · Power splitting ratio · Outage performance

1 Introduction

As one of the latest, most frontier and concerned technologies, the Fifth Generation (5G) is widely recognized as the key to realise the Internet of Everything (IoE). However, only limited number of the users can be served in the conventional multiple access schemes because of the limitation in the number of orthogonal resources blocks [1]. As a promising candidate, the non-orthogonal multiple

This work was supported by the National Natural Science Foundation of China (Grant No. 61601091), and the National Natural Science Foundation of China (Grant No. 61801093).

H. Song et al. (Eds.): SIMUtools 2019, LNICST 295, pp. 567–577, 2019.
https://doi.org/10.1007/978-3-030-32216-8_55

access (NOMA) has been received more and more attention recently [2,3]. The core idea of NOMA is that multiple users are multiplexed in the power-domain on the transmitter side and multi-user signal is seperated with a successive interference canceller (SIC) on the receiver side [2]. And in NOMA, it is an essential issue how to improve the data rate of the cell-edge user without doing harm to the Quality of Service (QoS) of the cell-center and the system. One possible solution to the issue is using cooperative transmission. Cooperative NOMA transmission was first proposed in [4], in which the cell-center user worked as a relay to improve the reception reliability of the cell-edge user. The author in [5] treated the decoding time of the cell-center user as a random variable and proposed a dynamic decode-and-forward based cooperative NOMA scheme with spatially random users, in which the outage performance of the system was improved. An another category of cooperative NOMA is the application of Simultaneous Wireless Information and Power (SWIPT) in NOMA, which was first proposed in [6]. The author in [7] proposed three cooperative transmission schemes utilizing hybrid SWIPT and antenna selection protocols to resolve the fairness issue of data rate between the cell-center user and the cell-edge user. In [8], the author invested a scenario where a user was in a poor channel and had to communicate with the base station with a dedicated relay. The SWIPT cooperative NOMA protocol was used in the relay and the author proposed an algorithm to get the optimal relaying transmission scheme to minimize the outage probability (OP) of the user. The author in [9] considered a downlink two-user NOMA where the SWIPT protocol was applied at the cell-center user. And the gradient decent method was used in the paper to find the optimal value of the PS ratio to maximize the sum-throughput of the system.

In this paper, we study a downlink two-user NOMA system, where one user can work as a relay to improve the OP of another user. Particularly, a dynamic SWIPT protocol is proposed and used at the cell-center user for cooperative transmission. In the DSWIPT NOMA scheme, both the power splitting (PS) and time allocation (TA) ratios can be adjusted dynamically. By this way, the fairness issue of data rate between the cell-center user and the cell-edge user can be solved without jeopardizing the sum-throughput of the system.

The rest of the paper is organized as follows. In Sect. 2, the system model for studying the dynamic SWIPT cooperative NOMA is introduced. In Sect. 3, the OP expressions of the cell-center user and the cell-edge user in the system are derived. And a joint optimization algorithm is proposed to maximize the sum-throughput of the system. In Sect. 4, numerical results are provided. Finally, Sect. 5 is the conclusion.

2 System Model

Figure 1 depicts a downlink two-user NOMA system, where a base station S communicates with a cell-center user $\mathrm{U_N}$ and a cell-edge user $\mathrm{U_F}$ simultaneously. Each node works in half-duplex mode. All wireless channels in the system follow independent and identically distributed (i.i.d) Rayleigh block flat fading. And the channels coefficient $h_{iv}(i \in \{\mathrm{S}, \mathrm{U_N}\}, v \in \{\mathrm{U_N}, \mathrm{U_F}\})$ between different nodes are constant during each transmission, where $|h_{iv}|^2$ is an exponential random variable with mean λ_{iv}. Additionally, the background noise n_i $(i \in \{\mathrm{U_N}, \mathrm{U_F}\})$ is a complex Gaussian random variable with mean zero and variance σ^2.

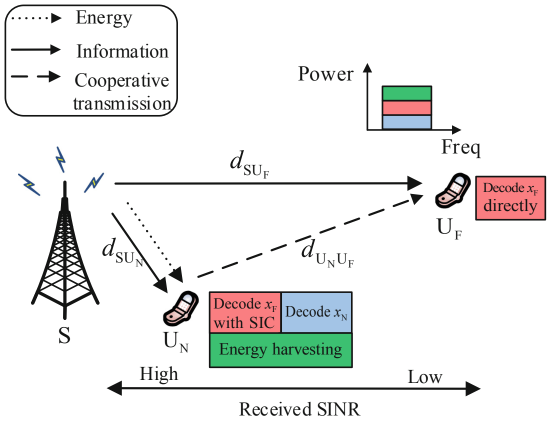

Fig. 1. Downlink two-user cooperative NOMA system model, which consists of a base station denoted by S and two paired users denoted by $\mathrm{U_N}$ and $\mathrm{U_F}$. SIC is performed at $\mathrm{U_N}$ to decode x_N.

To improve the outage performance of $\mathrm{U_F}$, we consider the application of SWIPT protocol at $\mathrm{U_N}$. The entire transmission period T can be divided into two phases. In the first phase, $\mathrm{U_N}$ harvests energy from received RF signals launched by S within the time $(1-\alpha)T$, where α $(0 < \alpha < 1)$ denotes the TA ratio. And the energy is simultaneously splitted for storing and information decoding with a ratio β and $1-\beta$, where β $(0 < \beta < 1)$ denotes the PS ratio. At the same time, $\mathrm{U_F}$ decodes information transmitted from S directly. In the second phase, within the time αT, $\mathrm{U_N}$ as a relay transmits signals to $\mathrm{U_F}$ with the full energy stored in the first phase if $\mathrm{U_N}$ has decoded the information successfully. At the meantime, $\mathrm{U_F}$ keeps performing information decoding by employing the selection combining (SC) technique [7]. Additionally, S keeps transmitting during the entire transmission period T.

According to the principle of NOMA, the message x_i $(i = \mathrm{N}, \mathrm{F})$ for $\mathrm{U_i}$ is coded in a superposition manner with a different power allocation coefficients $\sqrt{p_i}$ at S, where $E[x_i^2] = 1$. Here we assume $0 < p_\mathrm{N} < p_\mathrm{F} < 1$ and $p_\mathrm{N} + p_\mathrm{F} = 1$. At S, the coded message $\sqrt{p_\mathrm{N}} x_\mathrm{N} + \sqrt{p_\mathrm{F}} x_\mathrm{F}$ is transmitted with the power P_s during the entire transmission period. Hence, the received signal at $\mathrm{U_i}$ from S can be shown as

$$y_\mathrm{i} = (\sqrt{p_\mathrm{N} P_\mathrm{s}} x_\mathrm{N} + \sqrt{p_\mathrm{F} P_\mathrm{s}} x_\mathrm{F}) h_{\mathrm{SU_i}} d_{\mathrm{SU_i}}^{-l} + n_{U_i}, \tag{1}$$

where $h_{\mathrm{SU_i}}$ denotes the small-scale Rayleigh fading coefficient between S and $\mathrm{U_i}$ with $h_{\mathrm{SU_i}} \sim \mathcal{CN}(0,1)$, n_{U_i} denotes the additive white Gaussian noise (AWGN) at $\mathrm{U_i}$ with $n_i \sim \mathcal{CN}(0, \sigma^2)$, $d_{\mathrm{SU_i}}$ denotes the distance between S and $\mathrm{U_i}$, and l denotes the path loss exponent.

The power received by $\mathrm{U_N}$ is splitted up into two parts simultaneously. One part is used for information decoding with the ratio $1-\beta$, and the other part is used for energy storing with the ratio β. Hence, with the help of successive interference cancellation (SIC), the data rate at $\mathrm{U_N}$ for decoding x_i can be shown as

$$R_{\mathrm{N}}^{x_{\mathrm{F}}} = (1-\alpha)log_2(1+\frac{(1-\beta)p_{\mathrm{F}}P_{\mathrm{s}}|h_{\mathrm{SU_N}}|^2 d_{\mathrm{SU_N}}^{-l}}{(1-\beta)p_{\mathrm{N}}P_{rms}|h_{\mathrm{SU_N}}|^2 d_{\mathrm{SU_N}}^{-l}+\sigma^2}), \tag{2}$$

$$R_{\mathrm{N}}^{x_{\mathrm{N}}} = (1-\alpha)log_2(1+\frac{(1-\beta)p_{\mathrm{N}}P_{\mathrm{s}}|h_{\mathrm{SU_N}}|^2 d_{\mathrm{SU_N}}^{-l}}{\sigma^2}). \tag{3}$$

And the energy stored during the first phase at $\mathrm{U_N}$ can be shown as:

$$E_{\mathrm{N}} = (1-\alpha)T\eta\beta P_{\mathrm{s}}|h_{\mathrm{SU_N}}|^2 d_{\mathrm{SU_N}}^{-l}, \tag{4}$$

where η $(0<\eta<1)$ denotes the energy conversion efficiency of $\mathrm{U_i}$.

During the first phase, the received Signal to Interference plus Noise Ratio (SINR) at $\mathrm{U_F}$ for decoding x_{F} directly can be shown as

$$\gamma_{\mathrm{F}}^{x_{\mathrm{F}}} = \frac{p_{\mathrm{F}}P_{rms}|h_{\mathrm{SU_F}}|^2 d_{\mathrm{SU_F}}^{-l}}{p_{\mathrm{N}}P_{\mathrm{s}}|h_{\mathrm{SU_F}}|^2 d_{\mathrm{SU_F}}^{-l}+\sigma^2}. \tag{5}$$

If $\mathrm{U_N}$ has decoded x_{F} in the first phase, S and $\mathrm{U_N}$ will transmit message x_{F} to $\mathrm{U_F}$ synchronously during the second phase. If not, $\mathrm{U_N}$ keeps silence and S transmits alone. The transmission power of $\mathrm{U_N}$ can be shown as

$$P_{\mathrm{N}} = \frac{E_{\mathrm{N}}}{\alpha T} = (\frac{1-\alpha}{\alpha})\eta\beta P_{[\mathrm{s}]}|h_{\mathrm{SU_N}}|^2 d_{\mathrm{SU_N}}^{-l}. \tag{6}$$

At $\mathrm{U_F}$, the received signal from $\mathrm{U_N}$ can be shown as

$$y_{\mathrm{FN}} = \sqrt{P_{\mathrm{N}}}x_{\mathrm{F}}h_{\mathrm{U_N U_F}}d_{\mathrm{U_N U_F}}^{-l} + n_{U_{\mathrm{F}}}, \tag{7}$$

where $h_{\mathrm{U_N U_F}}$ denotes the small-scal Rayleigh fading coefficient between $\mathrm{U_N}$ and $\mathrm{U_F}$ with $h_{\mathrm{U_N U_F}} \sim \mathcal{CN}(0,1)$, $d_{\mathrm{U_N U_F}}$ denotes the distance between $\mathrm{U_N}$ and $\mathrm{U_F}$.

According to (6) and (7), with the help of $\mathrm{U_N}$, the received SINR at $\mathrm{U_F}$ for decoding x_{F} can be shown as

$$\gamma_{\mathrm{FN}}^{x_{\mathrm{F}}} = \frac{\eta\beta P_{\mathrm{s}}|h_{\mathrm{SU_N}}|^2|h_{\mathrm{U_N U_F}}|^2 d_{\mathrm{SU_N}}^{-l} d_{\mathrm{U_N U_F}}^{-l}(\frac{1-\alpha}{\alpha})}{\sigma^2}, \tag{8}$$

Finally, $\mathrm{U_F}$ selects signals with high SINR for reception. So the received SINR at $\mathrm{U_F}$ during the second phase can be written as

$$\gamma_{\mathrm{F}}^{sc} = \max\{\gamma_{\mathrm{F}}^{x_{\mathrm{F}}}, \gamma_{\mathrm{FN}}^{x_{\mathrm{F}}}\}. \tag{9}$$

Based on the signal reception model above, the data rate of $\mathrm{U_F}$ at the end of the transmission period can be expressed as

$$R_{\mathrm{F}}^{x_{\mathrm{F}}} = \begin{cases} (1-\alpha)log_2(1+\gamma_{\mathrm{F}}^{x_{\mathrm{F}}}) + \alpha log_2(1+\gamma_{\mathrm{F}}^{sc}) & R_{\mathrm{N}}^{x_{\mathrm{F}}} \geq R_{\mathrm{F}}^{th}, \\ log_2(1+\gamma_{\mathrm{F}}^{x_{\mathrm{F}}}) & R_{\mathrm{N}}^{x_{\mathrm{F}}} < R_{\mathrm{F}}^{th}, \end{cases} \tag{10}$$

where R_{F}^{th} denote the target data rate of decoding x_{F}.

3 Performance Analysis

3.1 Outage Performance

$\mathrm{U_N}$ will suffer a service outage when its data rate is below the target data rate. According to the principle of SIC, $\mathrm{U_N}$ should decode $\mathrm{U_F}$ first before decoding $\mathrm{U_N}$. So, the OP of $\mathrm{U_N}$ can be written as

$$P_{\mathrm{out}}^{\mathrm{N}} = \Pr(R_{\mathrm{N}}^{x_{\mathrm{F}}} < R_{\mathrm{F}}^{th}) + \Pr(R_{\mathrm{N}}^{x_{\mathrm{N}}} < R_{\mathrm{N}}^{th}, R_{N}^{x_{\mathrm{F}}} \geq R_{\mathrm{F}}^{th}), \tag{11}$$

where R_{F}^{th} and R_{N}^{th} denote the target data rates to decode x_{F} and x_{N}, respectively. And we also define $\gamma_{\mathrm{N},\alpha}^{x_{\mathrm{N}}} \triangleq 2^{\frac{R_{\mathrm{N}}^{th}}{1-\alpha}} - 1$, $\gamma_{\mathrm{N},\alpha}^{x_{\mathrm{F}}} \triangleq 2^{\frac{R_{\mathrm{F}}^{th}}{1-\alpha}} - 1$, $\varepsilon_1 \triangleq \frac{(1-\beta)p_{\mathrm{F}} P_{\mathrm{s}} d_{\mathrm{SU_N}}^{-l}}{\sigma^2}$, $\varepsilon_2 \triangleq \frac{(1-\beta)p_{\mathrm{N}} P_{[\mathrm{s}]} \mathrm{d}_{\mathrm{SU_F}}^{-1}}{\sigma^2}$, $\zeta \triangleq \frac{p_{\mathrm{F}}}{p_{\mathrm{N}}}$.

Theorem 1. *The closed form expression of the OP at* $\mathrm{U_N}$ *can be show as:*

$$P_{\mathrm{out}}^{\mathrm{N}} = \begin{cases} 1 - \min\{e^{-\mu_1}, e^{-\mu_2}\} & \alpha < 1-\nu, \\ 1 & \alpha \geq 1-\nu, \end{cases} \tag{12}$$

where $\mu_1 = \frac{\gamma_{\mathrm{N},\alpha}^{x_{\mathrm{F}}}}{\varepsilon_1 - \varepsilon_2 \gamma_{\mathrm{N},\alpha}^{x_{\mathrm{F}}}}$, $\mu_2 = \frac{\gamma_{\mathrm{N},\alpha}^{x_{\mathrm{F}}}}{\varepsilon_2}$, $\nu = \frac{R_{\mathrm{F}}^{th}}{log_2(1+\zeta)}$.

Proof. Define $X = |h_{\mathrm{SU_N}}|^2$. Plugging (2) and (3) into (11), the OP of $\mathrm{U_N}$ can be written as

$$P_{\mathrm{out}}^{\mathrm{N}} = \Pr(\frac{\varepsilon_1 X}{\varepsilon_2 X + 1} < \gamma_{\mathrm{N},\alpha}^{x_{\mathrm{F}}}) + \Pr(\varepsilon_2 X < \gamma_{\mathrm{N},\alpha}^{x_{\mathrm{N}}}, \frac{\varepsilon_1 X}{\varepsilon_2 X + 1} \geq \gamma_{\mathrm{N},\alpha}^{x_{\mathrm{F}}}). \tag{13}$$

For the case $\alpha \geq 1-\nu$, we obtain $(\varepsilon_1 - \varepsilon_2 \gamma_{\mathrm{N},\alpha}^{x_{\mathrm{F}}})X \leq 0$, so that the OP of $\mathrm{U_N}$ is always equal to 1. And for the case $\alpha < 1-\nu$, (11) can be written as

$$P_{\mathrm{out}}^{\mathrm{N}} = \Pr(X < \mu_1) + \Pr(X < \mu_2, X \geq \mu_1). \tag{14}$$

Based on the probability distribution of X and done by some algebraic manipulations, the OP expression of $\mathrm{U_N}$ can be shown in (12). And the proof of the Theorem 1 is completed. □

$\mathrm{U_F}$ will suffer a service outage when its data rate is below the target data rate. And the data rate of $\mathrm{U_F}$ depends on whether $\mathrm{U_N}$ decodes x_F successfully or not in the first phase. Based on (10), the OP of x_F can be written as

$$\begin{aligned} P_{\mathrm{out}}^{\mathrm{F}} = &\Pr((1-\alpha)log_2(1+\gamma_{\mathrm{F}}^{x_\mathrm{F}})+\alpha log_2(1+\gamma_{\mathrm{F}}^{sc})<R_{\mathrm{F}}^{th}, R_{\mathrm{N}}^{x_\mathrm{F}} \geq R_{\mathrm{F}}^{th}) \\ &+\Pr(log_2(1+\gamma_{F}^{x_\mathrm{F}})<R_{\mathrm{F}}^{th}, R_{\mathrm{N}}^{x_\mathrm{F}}<R_{\mathrm{F}}^{th}). \end{aligned} \tag{15}$$

In order to use the notations conveniently, we define $\Phi_i \triangleq cos(\frac{2i-1}{2I}\pi)$, $w_i \triangleq \frac{(1-\alpha)R_{\mathrm{F}}^{th}}{2}(\Phi_i+1)$, $\gamma_{w_i,\alpha} \triangleq 2^{\frac{w_i}{1-\alpha}}-1$, $\gamma_{w_i,\alpha}^{x_\mathrm{F}} \triangleq 2^{\frac{R_{\mathrm{F}}^{th}-w_i}{\alpha}}-1$, $\theta_1 \triangleq \frac{p_\mathrm{F} P s d_{\mathrm{SU_F}}^{-l}}{\sigma^2}$, $\theta_2 \triangleq \frac{p_\mathrm{N} P s d_{\mathrm{SU_F}}^{-l}}{\sigma^2}$, $\theta_3 \triangleq \frac{\eta\beta P s d_{\mathrm{SU_N}}^{-l} d_{\mathrm{U_N U_F}}^{-l}(\frac{1-\alpha}{\alpha})}{\sigma^2}$, $\kappa_1 \triangleq \frac{2^{R_{\mathrm{F}}^{th}}-1}{\theta_1-\theta_2(2^{R_{\mathrm{F}}^{th}}-1)}$.

Theorem 2. *The approximate expression of OP at* $\mathrm{U_F}$ *can be given as*

$$\begin{aligned} P_{\mathrm{out}}^{\mathrm{F}} \approx &\frac{(1-\alpha)R_{\mathrm{F}}^{th}}{2I}\sum_{i=1}^{I}\Big(\sqrt{1-\Phi_i^2}(1-\exp(-Q_3(\alpha,w_i))) \\ &\times(\exp(-\mu_1)(1-2\sqrt{Q_4(\alpha,w_i)})K_1(2\sqrt{Q_4(\alpha,w_i)})) \\ &\times\exp(-Q_1(\alpha,w_i))Q_2(\alpha,w_i)\Big)+(1-e^{-\kappa_1})(1-e^{-\mu_1}), \end{aligned} \tag{16}$$

where K_1 $(\cdot)$ is the modified Bessel function for the second kind, and

$$Q_1(\alpha,w_i)=\frac{\gamma_{w_i,\alpha}\sigma^2}{(p_\mathrm{F}-\gamma_{w_i,\alpha}p_\mathrm{N})Psd_{\mathrm{SU_F}}^{-l}}, \tag{17}$$

$$Q_2(\alpha,w_i)=\frac{2^w p_\mathrm{F}\sigma^2 ln2}{(p_\mathrm{F}-\gamma_{w_i,\alpha}p_\mathrm{N})^2 Psd_{\mathrm{SU_F}}^{-l}}, \tag{18}$$

$$Q_3(\alpha,w_i)=-\frac{\gamma_{w_i,\alpha}^{x_\mathrm{F}}}{\theta_1-\gamma_{w_i,\alpha}^{x_\mathrm{F}}\theta_2}, \tag{19}$$

$$Q_4(\alpha,w_i)=\frac{\gamma_{w_i,\alpha}^{x_\mathrm{F}}}{\theta_3}. \tag{20}$$

Proof. We define $W=(1-\alpha)log_2(1+\gamma_{\mathrm{F}}^{x_\mathrm{F}})$, $Y=|h_{\mathrm{SU_F}}|^2$, $Z=|h_{\mathrm{U_N U_F}}|^2$. And without loss of generality, we consider $W \leq (1-\alpha)R_{\mathrm{F}}^{th}$ [5].

The cumulative distribution function of random variable W can be shown as

$$F_W(w)=1-\exp(-\frac{\gamma_{w,\alpha}\sigma^2}{(p_F-\gamma_{w,\alpha}p_N)Psd_{\mathrm{SU_F}}^{-l}}). \tag{21}$$

Based on the cumulative distribution function $F_W(w)$, the Probability Density Function (PDF) of W can be shown as

$$f_W(w)=\exp(-\frac{\gamma_{w,\alpha}\sigma^2}{(p_\mathrm{F}-\gamma_{w,\alpha}p_\mathrm{N})Psd_{\mathrm{SU_F}}^{-l}})\frac{2^w p_\mathrm{F}\sigma^2 ln2}{(p_\mathrm{F}-\gamma_{w,\alpha}p_\mathrm{N})^2 Psd_{\mathrm{SU_F}}^{-l}}. \tag{22}$$

Secondly, we derive the OP of $\mathrm{U_F}$. Plugging (5), (9) and the random variable W into (15), the OP of $\mathrm{U_F}$ can be written as

$$\begin{aligned} P_{\text{out}}^{\text{F}} &= q_{\text{out}}^{\Psi_1} + q_{\text{out}}^{\Psi_2} \\ &= E_W(\mathrm{P}(\max\{\frac{\theta_1 Y}{\theta_2 Y+1}, XZ\theta_3\} < 2^{\frac{R_{\text{F}}^{th}-W}{\alpha}} - 1, \frac{\varepsilon_1 X}{\varepsilon_2 X+1} \geq \gamma_{\text{N},\alpha}^{x_{\text{F}}})) \\ &\quad + \mathrm{P}(\frac{\theta_1 Y}{\theta_2 Y+1} < 2^{R_{\text{F}}^{th}} - 1, \frac{\varepsilon_1 X}{\varepsilon_2 X+1} < \gamma_{\text{N},\alpha}^{x_{\text{F}}}). \end{aligned} \tag{23}$$

Done by some algebraic manipulations, $q_{\text{out}}^{\Psi_1}$ can be expressed as

$$\begin{aligned} q_{\text{out}}^{\Psi_1} = \int_0^{(1-\alpha)R_{\text{F}}^{th}} &(1-\exp(-\frac{\gamma_{w,\alpha}^{x_F}}{\theta_1 - \gamma_{w,\alpha}^{x_F}\theta_2})) \\ &\times (\exp(-\mu_1)(1-2\sqrt{\frac{\gamma_{w,\alpha}^{x_F}}{\theta_3}})K_1(2\sqrt{\frac{\gamma_{w,\alpha}^{x_F}}{\theta_3}}))f_W(w)dw, \end{aligned} \tag{24}$$

where $K_1(\cdot)$ is the modified Bessel function for the second kind.

The direct calculation of (24) will be very complicated. By using Gauss-Chebyshev quadrature, we approximate the expression (24) as

$$\begin{aligned} q_{\text{out}}^{\Psi_1} \approx &\frac{(1-\alpha)R_{\text{F}}^{th}}{2I} \sum_{i=1}^{I} \Big(\sqrt{1-\Phi_i^2}(1-\exp(-Q_3(\alpha,w_i))) \\ &\times (\exp(-\mu_1)(1-2\sqrt{Q_4(\alpha,w_i)})K_1(2\sqrt{Q_4(\alpha,w_i)})) \\ &\times \exp(-Q_1(\alpha,w_i))Q_2(\alpha,w_i)\Big), \end{aligned} \tag{25}$$

where $Q_1(\alpha,w_i)$, $Q_2(\alpha,w_i)$, $Q_3(\alpha,w_i)$ and $Q_4(\alpha,w_i)$ are defined as (17–20), respectively. And in (23), $q_{\text{out}}^{\Psi_2}$ can be written as

$$q_{\text{out}}^{\Psi_2} = (1-e^{-\kappa_1})(1-e^{-\mu_1}) \tag{26}$$

Thus, plugging (25) and (26) into (23), $P_{\text{out}}^{\text{F}}$ can be written as (16). The proof of the Theorem 2 is completed. □

3.2 Throughput Performance

In order to maximize the sum-throughput of the system, a joint optimization algorithm for selecting the TA ratio and the PS ratio is proposed in this subsection. Based on (12) and (16), the problem of maximizing the sum-throughput of the system can be expressed as

$$\begin{aligned} (\text{P1}):\max \quad & R_s(\alpha,\beta) = (1-P_{\text{out}}^{\text{N}})R_{\text{N}}^{th} + (1-P_{\text{out}}^{\text{F}})R_{\text{F}}^{th} \\ \text{s.t.} \quad & 0<\alpha<1, \\ & 0<\beta<1, \end{aligned} \tag{27}$$

which is a constrained optimization problem.

To solve this problem, we use the penalty function method to change the constrained optimization problem into the unconstrained optimization problem firstly. The penalty function can be expressed as

$$f(\alpha,\beta,r_k) = -R_s(\alpha,\beta) + r_k\left(\frac{1}{\alpha} + \frac{1}{1-\alpha} + \frac{1}{\beta} + \frac{1}{1-\beta}\right), \tag{28}$$

where r_k is a series of penalty factors which have decreasing property. Secondly, we use the pattern search method to solve the unconstrained optimization problem since it is hard to calculate the derivative of (28). The details of the proposed optimization algorithm can be summarized as Algorithm 1.

Algorithm 1. The algorithm of finding the optimal $(\alpha^\star, \beta^\star)$

Require: $P_\mathrm{s}, p_\mathrm{N}, p_\mathrm{F}, d_{\mathrm{SU_N}}, d_{\mathrm{SU_F}}, \eta, \sigma^2$ and $f(\alpha,\beta,r_k)$;

Initialization stopping threshold: ε_1, ε_2, interior-point: (α^0, β^0), obstacle factor: r_1, iteration index: k, shrinking coefficient: δ; initial step: ϑ_0, accelerated factor: τ, shrinking coefficient: ς, coordinate directions: $\boldsymbol{e_n}\,(n=2)$;
repeat
  $r_{k+1} = \delta r_k$; $i=1, j=1$, $\vartheta = \vartheta_0$; $\boldsymbol{x}^{(1)} = (\alpha^{(k)}, \beta^{(k)})$, $\boldsymbol{y}^{(1)} = \boldsymbol{x}^{(1)}$;
  repeat
    for $j = 1; j <\mathrm{n}; j++$ **do**
      if $f(\boldsymbol{y}^{(j)} + \vartheta \boldsymbol{e}_j) < f(\boldsymbol{y}^{(j)})$ **then**
        $\boldsymbol{y}^{(j+1)} = \boldsymbol{y}^{(j)} + \vartheta \boldsymbol{e}_j$;
      else if $f(\boldsymbol{y}^{(j)} - \vartheta \boldsymbol{e}_j) < f(\boldsymbol{y}^{(j)})$ **then**
        $\boldsymbol{y}^{(j+1)} = \boldsymbol{y}^{(j)} - \vartheta \boldsymbol{e}_j$;
      else
        $\boldsymbol{y}^{(j+1)} = \boldsymbol{y}^{(j)}$;
      end if
    end for
    if $f(\boldsymbol{y}^{(n+1)}) < f(\boldsymbol{x}^{(i)})$ **then**
      $\boldsymbol{x}^{(i+1)} = \boldsymbol{y}^{(n+1)}$; $\boldsymbol{y}^{(1)} = \boldsymbol{x}^{(i+1)} + \tau(\boldsymbol{x}^{(i+1)} - \boldsymbol{x}^{(i)})$; $i := i+1$, $j = 1$;
    else
      $\boldsymbol{y}^{(1)} = \boldsymbol{x}^{(i)}$; $\boldsymbol{x}^{(i+1)} = \boldsymbol{x}^{(i)}$; $\vartheta := \varsigma\vartheta$; $i := i+1$, $j = 1$;
    end if
  until $\vartheta < \varepsilon_2$. Update: $(\alpha^{(k+1)}, \beta^{(k+1)}) = \boldsymbol{x}^{i+1}$;
until $r_{k+1} B(\alpha^{(k+1)}, \beta^{(k+1)}) < \varepsilon_1$

4 Simulation Results

In this section, we compare the DSWIPT NOMA scheme with the NOMA scheme [2] and the SWIPT NOMA scheme [9]. The parameters are set up as: $R_\mathrm{N}^{th} = R_\mathrm{F}^{th} = 1$ bps/Hz; $p_\mathrm{N} = 0.1$, $p_\mathrm{F} = 0.9$; $n_\mathrm{N} = n_\mathrm{F} = -100$ dBm/Hz; bandwith $= 1$ MHz; $l = 3$; $\eta = 0.7$; $d_{\mathrm{SU_N}} = 2$ m, $d_{\mathrm{SU_F}} = 8$ m; $I = 30$. As can be seen

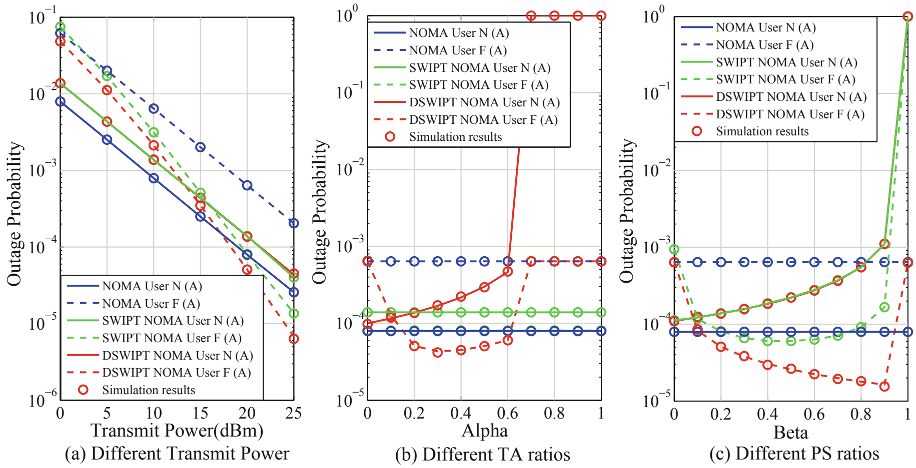

Fig. 2. Outage probability versus different transmit power, TA ratios and PS ratios.

from Fig. 2, the analytical results (A) are in exact accordance with Monte-Carlo simulation results, which corroborates our analyses in Sect. 3.

Figure 2 illustrates the OP versus different transmit power, TA ratios and PS ratios of the three schemes. In Fig. 2(a), we can see the OP of $\mathrm{U_F}$ in the DSWIPT NOMA scheme has been improved in comparison with that of $\mathrm{U_F}$ in [2] and [9]. In Fig. 2(b), we can see that α in the DSWIPT NOMA scheme can be adjusted according to the optimization algorithm proposed in Sect. 3 to maximize the sum-throughput of the system. And $\mathrm{U_N}$ will suffer a service outage and the outage performance of $\mathrm{U_F}$ will not be improved when α is higher than 0.7, which is because the decoding time of $\mathrm{U_N}$ is too short to decode x_{F} correctly. In Fig. 2(c), we can see $\mathrm{U_F}$ in the DSWIPT NOMA scheme has a lower OP comparing with that in [2] and [9]. And the outage performance of $\mathrm{U_F}$ in DSWIPT NOMA scheme is getting better as β going large.

Figure 3 provides the throughput performance versus the transmit power of the three schemes. In Fig. 3(a), the sum-throughput of the DSWIPT NOMA scheme and the sum-throughput of the NOMA scheme are similar and they are higher than that of the SWIPT NOMA scheme when the SNR is lower than 2.5 dbm. This is because the decoding time in the SWIPT NOMA scheme is short and can't be adjusted flexible, which has a significant influence on the OP of $\mathrm{U_N}$. As can be seen in Fig. 3(b), the DSWIPT NOMA scheme has a better performance in the throughput of $\mathrm{U_F}$ comparing with the other two schemes, which illustrates the DSWIPT NOMA scheme indeed improves the OP of $\mathrm{U_F}$ even though the SNR is low. Thus, the throughput gap between the cell-center user and the cell-edge user can be reduced with the DSWIPT NOMA scheme.

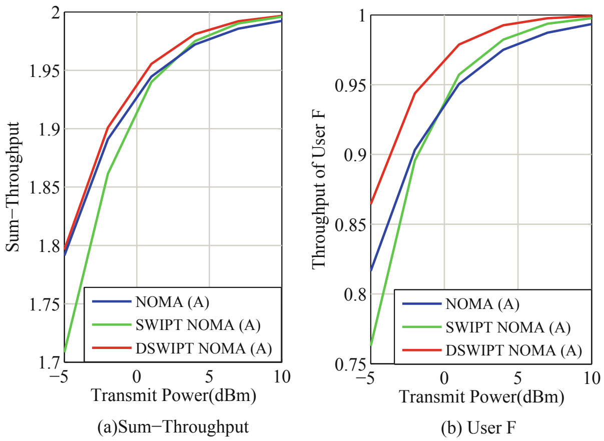

Fig. 3. Throughput of the system and U_F versus the Transmit SNR.

5 Conclusion

In this paper, we focus on the issue of throughput fairness between the cell-center user and the cell-edge user in a downlink two-user NOMA system. We have proposed the DSWIPT NOMA scheme and have investigated the outage performance and the throughput performance of the users in the scheme. And we have also proposed an optimization algorithm to get the maximal sum-throughput of the DSWIPT NOMA scheme. The numerical results have illustrated that the throughput performance of the cell-edge user can be enhanced quite a lot without jeopardizing the sum-throughput of the downlink two-users NOMA system when using the DSWIPT NOMA scheme. Consequently, we can say that the DSWIPT NOMA scheme is a significant solution for the issues like fairness in throughput performance between different users.

References

1. ITU-R M.2083, IMT vision–Framework and overall objectives of the future development of IMT for 2020 and beyond. https://www.itu.int/rec/R-REC-M.2083. Accessed 10 June 2018
2. Saito, Y., Kishiyama, Y., Benjebbour, A., Nakamura, T., Li, A., Higuchi, K.: Non-orthogonal multiple access (NOMA) for future radio access. In: 2013 IEEE 77th Vehicular Technology Conference (VTC Spring), Dresden, Germany, pp. 1–5 (2013)
3. Cai, Y., Qin, Z., Cui, F., Li, G.Y., McCann, J.A.: Modulation and multiple access for 5G networks. IEEE Commun. Surv. Tutorials **20**(1), 629–646 (2018)
4. Ding, Z., Peng, M., Poor, H.V.: Cooperative non-orthogonal multiple access in 5G systems. IEEE Commun. Lett. **19**(8), 1462–1465 (2015)
5. Zhou, Y., Wong, V.W.S., Schober, R.: Dynamic decode-and-forward based cooperative NOMA with spatially random users. IEEE Trans. Wirel. Commun. **17**(5), 3340–3356 (2018)

6. Liu, Y., Ding, Z., Elkashlan, M., Poor, H.V.: Cooperative non-orthogonal multiple access with simultaneous wireless information and power transfer. IEEE J. Sel. Areas Commun. **34**(4), 938–953 (2016)
7. Do, T.N., da Costa, D.B., Duong, T.Q., An, B.: Improving the performance of cell-edge users in MISO-NOMA systems using TAS and SWIPT-based cooperative transmissions. IEEE Trans. Green Commun. Netw. **2**(1), 49–62 (2018)
8. Ye, Y., Li, Y., Wang, D., Zhou, F., Hu, R.Q., Zhang, H.: Optimal transmission schemes for DF relaying networks using SWIPT. IEEE Trans. Veh. Technol. **67**(8), 7062–7072 (2018)
9. Do, T.N., An, B.: Optimal sum-throughput analysis for downlink cooperative SWIPT NOMA systems. In: 2018 2nd International Conference on Recent Advances in Signal Processing, Telecommunications Computing (SigTelCom), pp. 85–90 (2018)